

**Lévy-noise-induced transport in a rough triple-well potential**Yongge Li,<sup>1,2</sup> Yong Xu,<sup>1,\*</sup> Jürgen Kurths,<sup>2,3</sup> and Xiaole Yue<sup>1</sup><sup>1</sup>*Department of Applied Mathematics, Northwestern Polytechnical University, Xi'an 710072, China*<sup>2</sup>*Potsdam Institute for Climate Impact Research, Potsdam 14412, Germany*<sup>3</sup>*Institute of Applied Physics of the Russian Academy of Sciences, 603950 Nizhny Novgorod, Russia*

(Received 15 June 2016; published 26 October 2016)

Rough energy landscape and noisy environment are two common features in many subjects, such as protein folding. Due to the wide findings of bursting or spiking phenomenon in biology science, small diffusions mixing large jumps are adopted to model the noisy environment that can be properly described by Lévy noise. We combine the Lévy noise with the rough energy landscape, modeled by a potential function superimposed by a fast oscillating function, and study the transport of a particle in a rough triple-well potential excited by Lévy noise, rather than only small perturbations. The probabilities of a particle staying in the middle well are considered under different amplitudes of roughness to find out how roughness affects the steady-state probability density function. Variations in the mean first passage time from the middle well to the right well have been investigated with respect to Lévy parameters and amplitudes of the roughness. In addition, we have examined the influences of roughness on the splitting probabilities of the first escape from the middle well. We uncover that the roughness can enhance significantly the first escape of a particle from the middle well, especially for different skewness parameters, but weak differences are found for stability index and noise intensity on the probabilities a particle staying in the middle well and splitting probability to the right.

DOI: [10.1103/PhysRevE.94.042222](https://doi.org/10.1103/PhysRevE.94.042222)**I. INTRODUCTION**

The transports of a random particle on an energy landscape hold the key to understanding a wide range of molecular or atom phenomena and can be considered historically important. Usually in these problems the underlying potential profile is considered to be constant or at least regular. However, a typical example in protein folding shows that the potential surface of a protein may have a hierarchical structure with potential minima within potential minima, which means the underlying energy landscapes can be spatially rough due to multiple energy scales associated with the building blocks of proteins [1,2]. Similar rough energy landscape structure has also been found in many other fields like the activation gating of ion channels [3,4], diffusions in structural glasses [5,6], and supercooled liquids [7,8]. In a seminal paper by Zwanzig [9], he first modeled the rough energy landscape by superimposing a fast-oscillating trigonometric function on the background energy potential function, which is now widely adopted and applied in protein dynamics by many scholars [10–13]. And thus a problem is raised that how roughness on a potential surface affects the dynamical behaviors opening to a random environment.

Despite the broad applicability and importance of the rough energy landscape, the overwhelming majority of studies of the underlying stochastic dynamics have concentrated on smooth potential models in subjects of stochastic resonance [14,15], coherence resonance [16,17], stochastic bifurcations [18,19], and noise-induced transitions [20,21], and it has several applications [22–25]. As a result, there are surprisingly few theoretical studies of this problem leading to little knowledge about the effects of roughness at a quantitative level. In the presence of rough potential, the transports of a particle may become significantly different, because the multiple maxima

and minima of roughness can provide temporary stopovers on the steep potential wall for a short stay. Zwanzig obtained an equivalent potential and an effective diffusion coefficient, indicating that the roughness of a potential gives rise to a dramatic slowing down of diffusion at low temperatures [9]. Mondal *et al.* found that an increase of roughness can lead to a remarkable suppression of the probability current in a one-dimensional ratchet potential for a Brownian particle [26]. Different from trigonometrically described roughness, another universally used irregular potential is the random potential [27–29]. The differences between a random potential and a rough potential lie in the fact that the former has a disordered potential and a single spatial scale, while the latter is relatively regular but involves more than one distinct scale.

The dynamics of Brownian particles is already well understood since Einstein's seminal paper, and has found applications in various fields [30–33]. However, evidences show that random environment in gene regulation, laser gyroscope, and millennial climate changes exhibits bursting phenomenon [34–36], in which Gaussian noise is bounded on modeling this kind of noise. A typical example in gene expression shows that transcription often occurs in bursts rather than at a constant rate, so Poisson noises are added into the genetic circuit to make up the shortage of Gaussian perturbations [37,38]. While Lévy noise consists of small perturbations and large jumps, which turns out to be a relatively proper tool to describe this environment, and some applications appear in the investigations of *Escherichia coli* walk, light wave trajectories, and some aspects of earthquake behaviors [39–41].

So we believe the combination of rough potentials and Lévy noise will be inspiring and meaningful to the study of protein-related dynamics. The main objective in this paper is to explore the influences of roughness on the transports of a particle (assume no interactions with other particles) excited by Lévy noise in a triple-well system. As stated the existence of roughness will provide particles with lots of small

\*Corresponding author: [hsux3@nwpu.edu.cn](mailto:hsux3@nwpu.edu.cn)

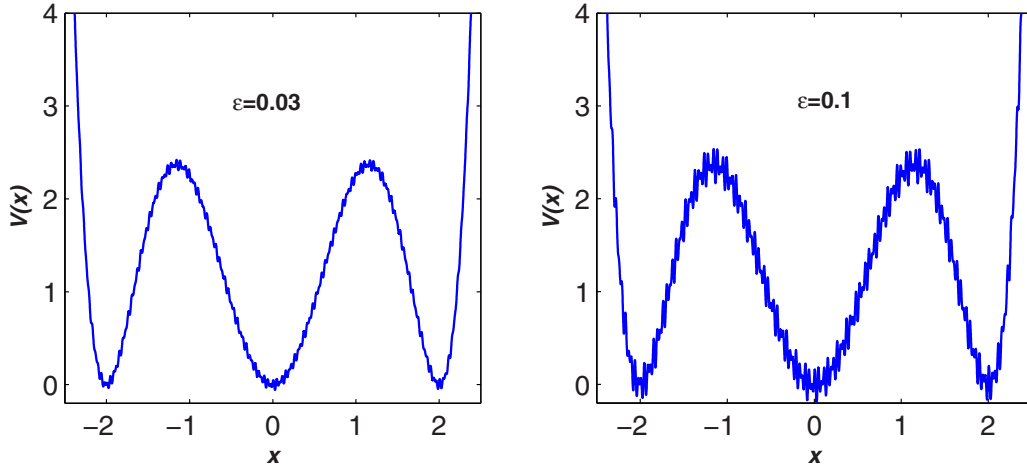


FIG. 1. Diagrams illustrating of the rough potential Eq. (2) for different  $\varepsilon$ .

stopovers for a temporary stay, which definitely influences a lot on the transport processes. As a result, we ask whether the roughness will affect the probability distribution, how it influences the barrier crossing process, and what will happen under excitations mixing large jumps with small perturbations.

With the above questions, we arrange the paper as follows: in Sec. II, we introduce a rough potential model subject to Lévy noise. In Sec. III, the steady-state probability density function is computed to examine the influences of roughness and Lévy parameters. In Sec. IV, we explore how roughness affects the mean first passage time (MFPT) under different Lévy parameters. Section V is devoted to investigating the splitting probability under the rough potential. The paper is concluded in Sec. VI.

## II. THE MODEL

Consider a particle unaffected by other particles embedded in a triple well potential  $V(x)$  in the presence of Lévy stable noise, and the Langevin equation of the particle takes the following form:

$$\dot{x}(t) = -V'(x) + \dot{L}(t), \quad (1)$$

where the overdot is the derivative of time and the prime denotes the spatial derivative.  $V(x)$  contains a general smooth background  $V_0(x)$  on which a rapidly oscillating perturbation  $V_1(x)$  is superimposed, so that  $V(x) = V_0(x) + V_1(x)$ . In this work we analyze

$$\begin{aligned} V_0(x) &= x^2(0.5x^2 - 2)^2, \quad V_1(x) \\ &= \varepsilon(\sin \omega_1 x + \cos \omega_2 x), \quad \varepsilon \ll 1, \end{aligned} \quad (2)$$

where  $\varepsilon$  is a measure of the amplitude of roughness on the potential. The frequencies  $\omega_1$  and  $\omega_2$  control the density of roughness. An illustration is shown in Fig. 1, we set  $\omega_1 = 173$  and  $\omega_2 = 119$ , which holds in the whole context.  $V_0(x)$  is a smooth symmetric triple well potential, with two maxima  $x_{\max}^{\pm} = \pm 1.1547$  and three minima at  $x_{\min} = 0, x_{\min}^{\pm} = \pm 2.0$ . The potential becomes rugged when the roughness is superimposed, with potential minima within potential minima, which is stronger with the increase of  $\varepsilon$ .

$L(t)$  is a Lévy stable motion, for  $0 < \alpha \leq 2, \alpha \neq 1$  the characteristic function of  $L(t)$  takes the form

$$E[e^{ikL(t)}] = \exp\left[-tD|k|^\alpha \left(1 - i\beta \text{sgn}k \tan \frac{\pi\alpha}{2}\right)\right], \quad (3)$$

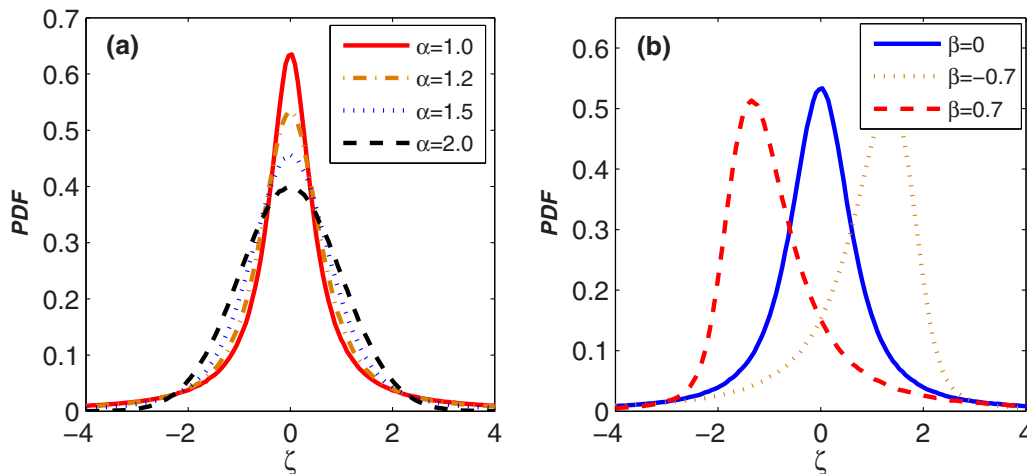


FIG. 2. The probability density functions (PDFs) of Lévy noise. (a)  $\beta = 0, D = 0.5$ , (b)  $\alpha = 1.2, D = 0.5$ .

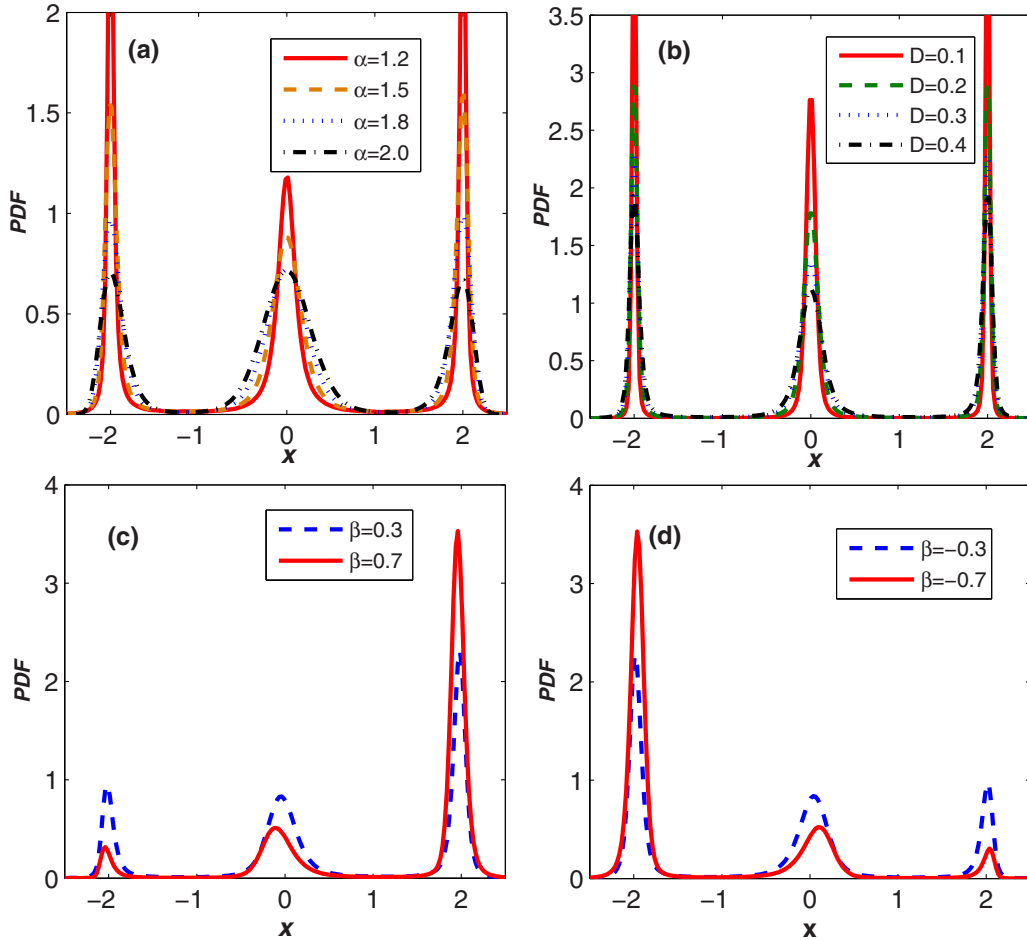


FIG. 3. The PDFs for different Lévy parameters. (a)  $\beta = 0$ ,  $D = 0.3$ , the larger is  $\alpha$  the fatter is the PDF. (b)  $\alpha = 1.5$ ,  $\beta = 0$ , the changes are similar with  $\alpha$ , but PDFs for different  $D$  are always slim. (c)  $\alpha = 1.5$ ,  $D = 0.3$ , for  $\beta > 0$  the PDFs are right-skewed, for  $\beta < 0$  the PDFs are left-skewed.

where  $\alpha$  is the stability index,  $\beta$  ( $-1 \leq \beta \leq 1$ ) is the skewness parameter, and  $D = c^\alpha$  denotes the noise intensity, and  $c$  is the scale parameter [42]. A set of Lévy distributions with respect to different parameters are presented in Fig. 2 to illustrate their heavy-tailed and skewed properties. Obviously,  $\alpha$  affects the thickness of the tail (the distribution is Gaussian for  $\alpha = 2$ ), that smaller  $\alpha$  generate heavier tails and more large jumps.  $\beta$  is used to measure the symmetry of the noise, when  $\beta = 0$  the distribution is symmetric. Under the condition of  $1 < \alpha < 2$ , for  $\beta > 0$  the PDF is left-skewed with a heavy right tail to balance the mean value zero, while for  $\beta < 0$  it is right-skewed. In this paper, we restrict our interest on the region  $1 < \alpha \leq 2$  throughout the paper.

### III. STEADY-STATE DISTRIBUTIONS

The PDF is one of the most popular mathematic tools to describe stochastic dynamics. During the past several decades, analytical theories, such as FPE, Smoluchowski equation, and stochastic Liouville equation [43], have been proposed under the background of Gaussian noise to derive the PDFs. The efficiency was affirmed by numerical simulations from analytically solvable cases. However, FPE corresponding

to Lévy-noise-induced systems is fractional-order on the diffusion term, with the form

$$\frac{\partial}{\partial t} p = \frac{\partial}{\partial x} (V' p) + D \frac{\partial^\alpha p}{\partial |x|^\alpha}, \quad (4)$$

corresponding to system Eq. (1), where  $\partial^\alpha / \partial |x|^\alpha$  is the fractional Riesz derivative [44]. When  $\alpha = 2$  it reduces to the normal FPE. However, although the form of fractional FPE can be given, rare types can be solved analytically even for one-dimensional systems, except some special cases, which is further difficult for rough potential systems. So in this manuscript, Monte Carlo simulations are applied directly. Before addressing the results, we present the numerical discrete form, at times  $t_n = n\Delta t$ ,  $n = 0, 1, 2, \dots$  for a sufficiently small time step  $\Delta t$ ,

$$x_{n+1} = x_n - V'(x_n)\Delta t + (\Delta t)^{1/\alpha} \xi_{\alpha, \beta, D}(n), \quad (5)$$

where  $\xi_{\alpha, \beta, D}(n)$  is the Lévy random number with triple  $(\alpha, \beta, D)$ . To highlight the influences of the roughness, we set the integration step time  $\Delta t$  smaller than  $10^{-4}$  and the stochastic averages reported below over  $2 \times 10^5$  trajectories with initial locations at the bottom of the middle well.

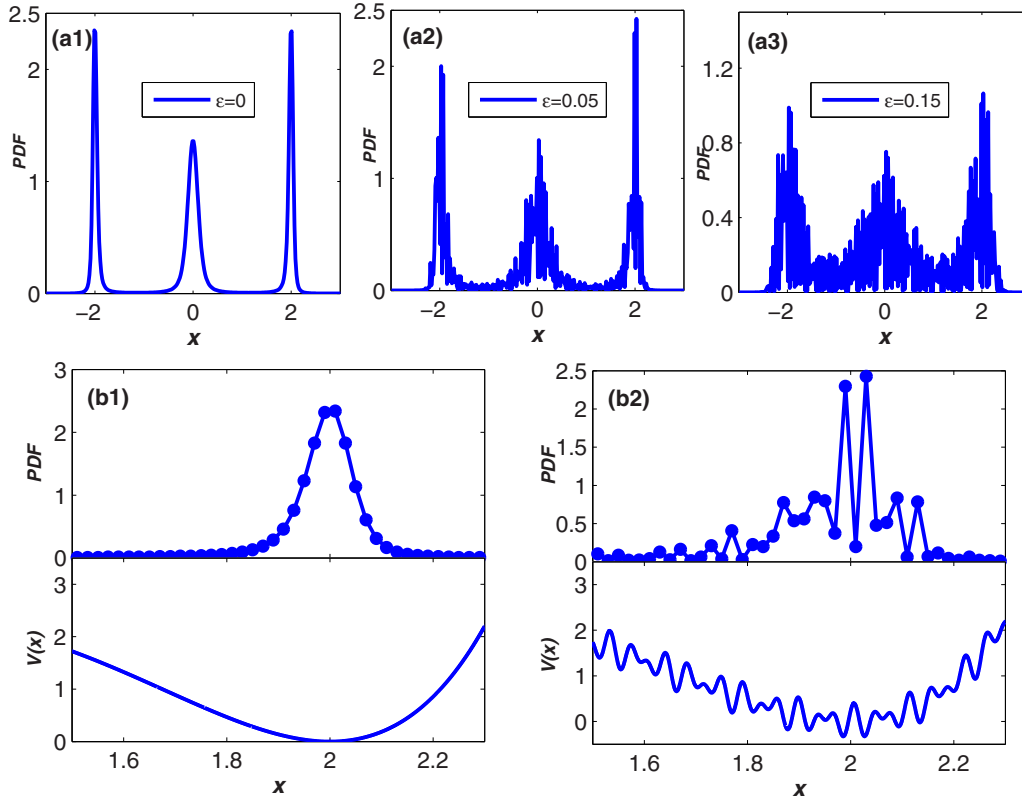


FIG. 4. The PDFs for different amplitudes of roughness in the potential under the parameters  $\alpha = 1.5$ ,  $D = 0.3$ . (a) Plots of PDFs for  $\varepsilon$  varying from zero to 0.15. (b) Comparisons of the PDFs in the region (1.5, 2.3) for  $\varepsilon = 0$  and  $\varepsilon = 0.05$  corresponding to their potentials.

PDFs in the absence of roughness are given in Fig. 3. We show that when  $\beta = 0$  the variation of  $\alpha$  and  $D$  will not break the symmetry of the PDFs. For small  $\alpha$  the PDFs are slim and high, with the increase of  $\alpha$  the shapes of the PDFs become fatter, and tend to the dumpy state like Gaussian noise  $\alpha = 2$ . This is because, when there is no noise, a particle will stay at the bottom of the middle well and tend to  $x = 0$  with  $x_n - V'(x_n)\Delta t \approx 0$ . When noise is added in the system, after one step iteration  $x_{n+1} \approx (\Delta t)^{1/\alpha} \xi_{\alpha, \beta, D}(n)$ , then if the system happens to encounter a large Lévy noise  $|(\Delta t)^{1/\alpha} \xi_{\alpha, \beta, D}(n)| > x_{\max}^+$ , the particle will jump to other wells easily, but if it is a small excitation, several more homodromous excitations are needed to jump to other wells. So for small  $\alpha$ , large jumps play a leading role, but as  $\alpha$  increases small fluctuations overtake slowly. So we see heavier-tailed Lévy noises induce slimmer PDFs, while larger  $\alpha$  induce fatter PDFs. The effects of the intensity  $D$  can be seen in Eq. (5), which influences the dynamics by linearly increasing the noise part:  $(\Delta t)^{1/\alpha} \xi_{\alpha, \beta, D}(n) \sim D^{1/\alpha} [(\Delta t)^{1/\alpha} \xi_{\alpha, \beta, 1}(n)]$ .

Different from  $\alpha$  and  $D$ ,  $\beta$  affects the symmetry. It is clearly shown in Figs. 3(c) and 3(d) that for  $\beta > 0$ , the PDFs are right-skewed, while for  $\beta < 0$ , they are left-skewed, which is exactly opposite to the right-skewed distribution of Lévy noise stated above. Because for  $\beta > 0$ , although the Lévy distribution is left-skewed, it has a heavy tail in the right-hand side, then vast numbers of positive large jumps make it much easier for a particle to transfer from the middle well to the right well. In addition, when a particle jumps to the right well, for the lack of minus large excitations, it is difficult for it to

return back to the middle or left well, so we see the right well occupies the most parts of the probability.

When roughness is imposed on the smooth potential  $V_0(x)$ , the direct influences on the PDFs are shown in Fig. 4. In intuitional senses, the PDFs change from smooth to rugged and the phenomenon becomes intenser with the increase of  $\varepsilon$ . Region (1.5, 2.3) is shown in detail to compare the fluctuations of PDFs corresponding to the rough potential. In the smooth case, particles can hardly stay on the potential wall for a while, but thanks to the small minima within the steep wall, they are able to stay on the wall and oscillate in these small rough wells for a short time, and so the PDFs become rugged.

Despite the visual results, we are concerned about the quantitative influences on the probability in each well. Therefore, without loss of generality, we measure the probability that a particle stays in the middle well by integrating the PDF:

$$P_{\text{mid}} = \int_{x_{\max}^-}^{x_{\max}^+} p(x) dx. \quad (6)$$

It should be claimed that although roughness changes the maximum and minimum of the potential, we define the middle well as region  $(x_{\max}^-, x_{\max}^+)$  to keep coincident with the smooth case.

Figure 5 shows how  $\varepsilon$  and  $\alpha$ ,  $\beta$ ,  $D$  affect  $P_{\text{mid}}$ . For  $\alpha$  and  $D$ , we find that the differences keep small for different  $\varepsilon$  in Figs. 5(a) and 5(b), which means that the influences of roughness on  $P_{\text{mid}}$  are not significant with respect to  $\alpha$  and  $D$ . However, it is very different for  $\beta$ . With an increase of  $\beta$

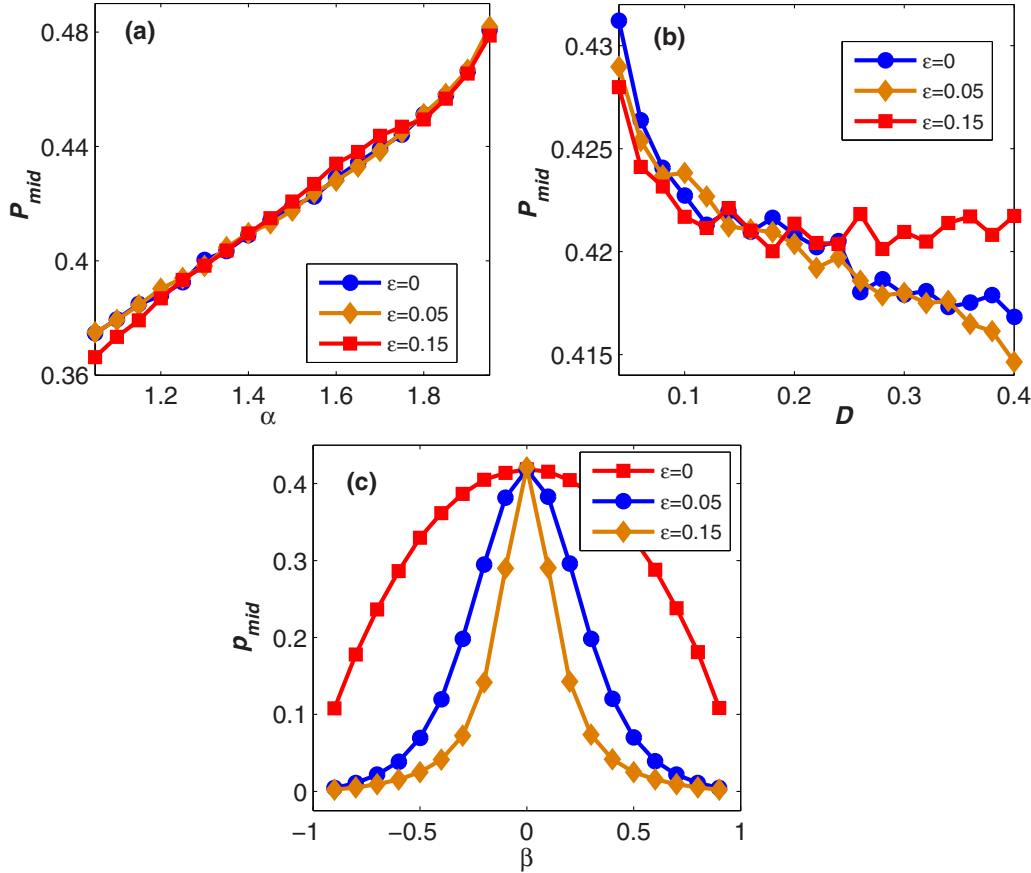


FIG. 5.  $P_{mid}$  for different amplitudes of roughness with respect to  $\alpha$ ,  $D$ , and  $\beta$ , (a)  $\beta = 0$ ,  $D = 0.3$ ,  $P_{mid}$  increases with  $\alpha$ , but the differences between different roughness are small. (b)  $\alpha = 1.5$ ,  $\beta = 0$ ,  $P_{mid}$  decreases along with the noise intensity  $D$  in the absence of roughness, when  $\varepsilon = 0.15$   $P_{mid}$  tends to relatively stationarily for large  $D$ . (c)  $\alpha = 1.5$ ,  $D = 0.3$ ,  $P_{mid}$  is almost symmetric around  $\beta = 0$ , and the roughness decreases  $P_{mid}$  significantly.

from -1 to 1  $P_{mid}$  goes through increasing and decreasing two stages. When  $|\beta|$  is close to 1,  $P_{mid}$  is very small, which says a particle hardly stays in the middle well. This phenomenon can be explained as follows: taking the right axis, for example, when  $\beta > 0$  the heavy right tail of Lévy distribution can easily kick particles out of the middle well, when they try to go back to the middle well, numerous large positive excitations will probably pull them back. Fixing  $\beta$ , the decreasing of  $P_{mid}$ , resulting from the increase of  $\varepsilon$ , clearly shows significant effects of roughness with respect to  $\beta$ . Compared with  $\alpha$  and  $D$ , we find that a skewed Lévy noise is more sensitive to the roughness, which can amplify the effect of skewness parameter  $\beta$ , and the larger  $\varepsilon$  is, the stronger this effect is. In the next section, we will see how  $\varepsilon$  enhances the phenomenon.

**IV. MFPT FROM THE MIDDLE TO THE RIGHT**

A particle inserted into the middle well will spend a random time within this well until it encounters a large spike or several continuous small one-direction diffusions and kicks it out of the well, which can be described as the FPT to measure the duration of a particle escaping from the potential well. An average imposed on FPT is the MFPT in the statistical sense. In this part we study the MFPT from the middle well to the right well (the regime is the same with the left well), and both

cases  $\varepsilon = 0$  and  $\varepsilon \neq 0$  are computed to illustrate the influences of the roughness. In these simulations, a particle starts from the bottom of the middle well and proceeds until it reaches or crosses the boundary defined at the bottom of the right well,  $x = 2.0$ , and then restarts Eq. (5) until the procedure is performed more than  $2 \times 10^5$  times for one fixed point. To ensure particles really transfer to the right well, we define the FPT as follows:

$$\tau(x_{right}) = \inf\{t : x(t) > x_{min}^+\}. \tag{7}$$

Taking an average on the FPT generates the MFPT:

$$MFPT = \langle \tau(x_{right}) \rangle. \tag{8}$$

When  $\varepsilon = 0$  in Fig. 6, with the increase of  $\alpha$  particles need more time to escape from the middle well, while  $\beta$  and  $D$  perform oppositely. Because larger  $\alpha$  means less large Lévy excitations, while larger  $|\beta|$  indicates more large biased excitations, and it is obvious that the increase of  $D$  will promote particles to escape from the middle well.

Figure 7 clearly shows how the roughness affects the MFPTs for different  $\alpha$ ,  $\beta$ , and  $D$ . It is an interesting phenomenon that the roughness does not prevent particles from crossing barriers but promotes the process. This phenomenon attributes to the fact as follows. When a particle starts from the bottom of the middle well, if it wants to cross the right barrier

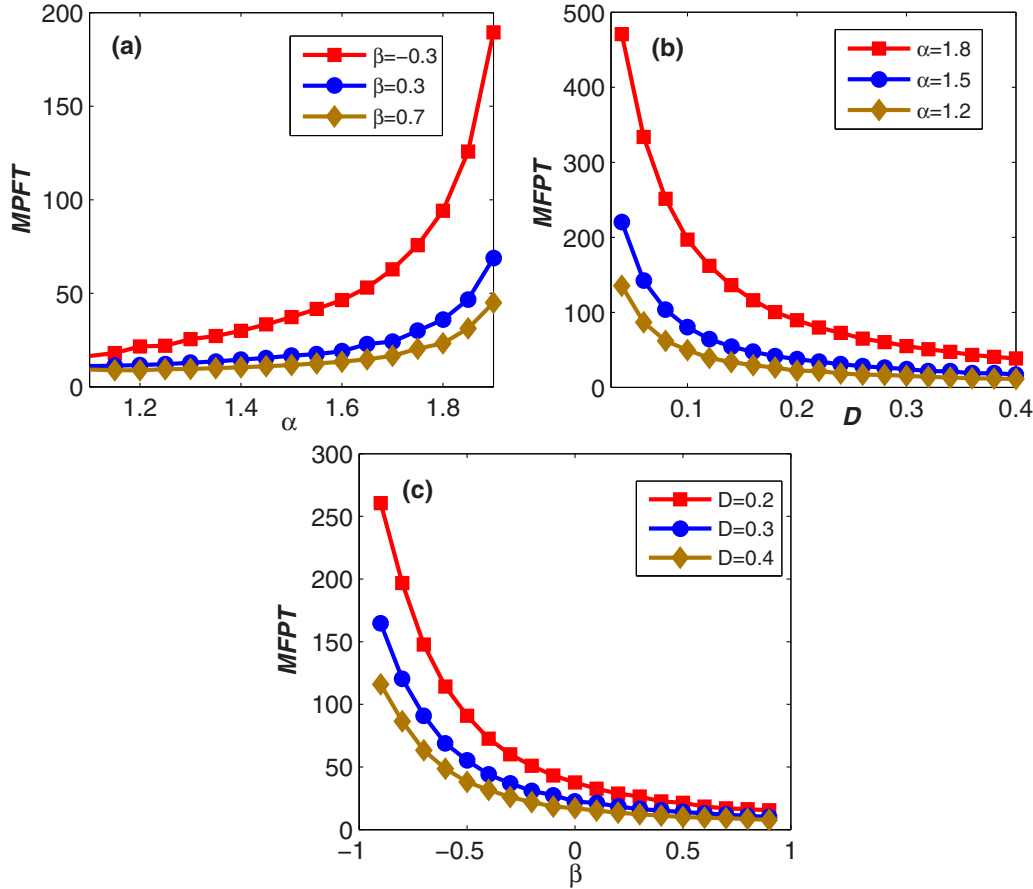


FIG. 6. MFPTs in the absence of roughness ( $\epsilon = 0$ ) with respect to  $\alpha$ ,  $D$ , and  $\beta$ . (a)  $D = 0.3$ , with the increase of  $\alpha$  particles need more and more time to escape. (b)  $\beta = 0$ , large  $D$  will decrease the MFPT of particles. (c)  $\alpha = 1.5$ , the increase of  $\beta$  can promote the escape of particles.

and reach the right well bottom  $x_{\min}^+$  at one shot, it at least needs an excitation  $(\Delta t)^{1/\alpha} \xi_{\alpha, \beta, D}(n) \geq x_{\min}^+$ . But if a particle is able to stay at the halfway  $x_{sw}$  on the potential wall for a while and starts from there, it just needs an excitation  $(\Delta t)^{1/\alpha} \xi_{\alpha, \beta, D}(n) \geq (x_{\min}^+ - x_{sw})$ . In fact, the roughness produces a ladder-like platform, leading particles a short stay at somewhere on the steep walls, and wait for excitations relatively much smaller than  $x_{\min}^+$  to kick particles out, while in the smooth potential case, particles will return to the bottom quickly if there are no continuous positive excitations. So the roughness enables particles to use a wider band of Lévy excitations and decreases the recovery rate to the bottom, which probably helps particles to get enough time to wait for a critical excitation. In addition, despite those one-shot crossings, when excitations are small, the process likes a relay race, in which the ladders provide lots of temporary relay points and enable one after another small excitation to transfer particles to other points, and finally small excitations step-by-step accomplish crossing work by two, three, or more hits as illustrated in Fig. 8. During the process, particles from  $x_{\min} = 0$  to  $x_{\min}^+ = 2.0$ , should experience the uphill and downhill stage, which will accelerate and retard particles to get to another well, respectively. In the smooth case, particles will slide down to the right bottom quickly when they cross  $x_{\max}^+$ , but when roughness is imposed the process slows down. However, the downhill distance is  $x_{\min}^+ -$

$x_{\max}^+ = 0.8453$ , which is smaller than the climbing distance  $x_{\max}^+ - x_{\min} = 1.1547$ . So in one sense, the total effect is that MFPTs decrease under the interference of roughness. On this basis, we see roughness is indeed beneficial to the crossing.

Furthermore, it seems that large  $\alpha$  and small  $D$  induce a larger accelerating range. To illustrate these effects, we define a tool to measure the degree of roughness upon MFPTs,

$$\rho = \frac{\text{var}(\tau)}{\tau_{\epsilon=0}}, \quad (9)$$

where  $\text{var}(\tau)$  measures how far the set of computed MFPTs spread out, and the denominator  $\tau_{\epsilon=0}$  describes the level of MFPT in the absence of roughness. Then we get  $\rho_{\alpha=1.2} = 0.002$ ,  $\rho_{\alpha=1.5} = 0.098$ ,  $\rho_{\alpha=1.8} = 0.509$  in Fig. 7, which means that larger  $\alpha$  get more influences. This is because small perturbations need to take advantage of these rugged barriers, while large excitations can kick particles out by one or two hits and thus benefit less from the roughness, so more small excitations get more influences. As shown in Sec. II, large  $\alpha$  have fat inverse bell-like distributions of which small excitation takes up the most percent, so they get more influences on the MFPTs. Because  $D$  is to adjust the amplitude of noise linearly,  $D^{1/\alpha} [(\Delta t)^{1/\alpha} \xi_{\alpha, \beta, 1}(n)]$ , so  $D$  generates similar phenomena as  $\alpha$  under the roughness, like  $\rho_{D=0.1} = 0.466$ ,  $\rho_{D=0.2} = 0.201$ , and  $\rho_{D=0.4} = 0.057$ .

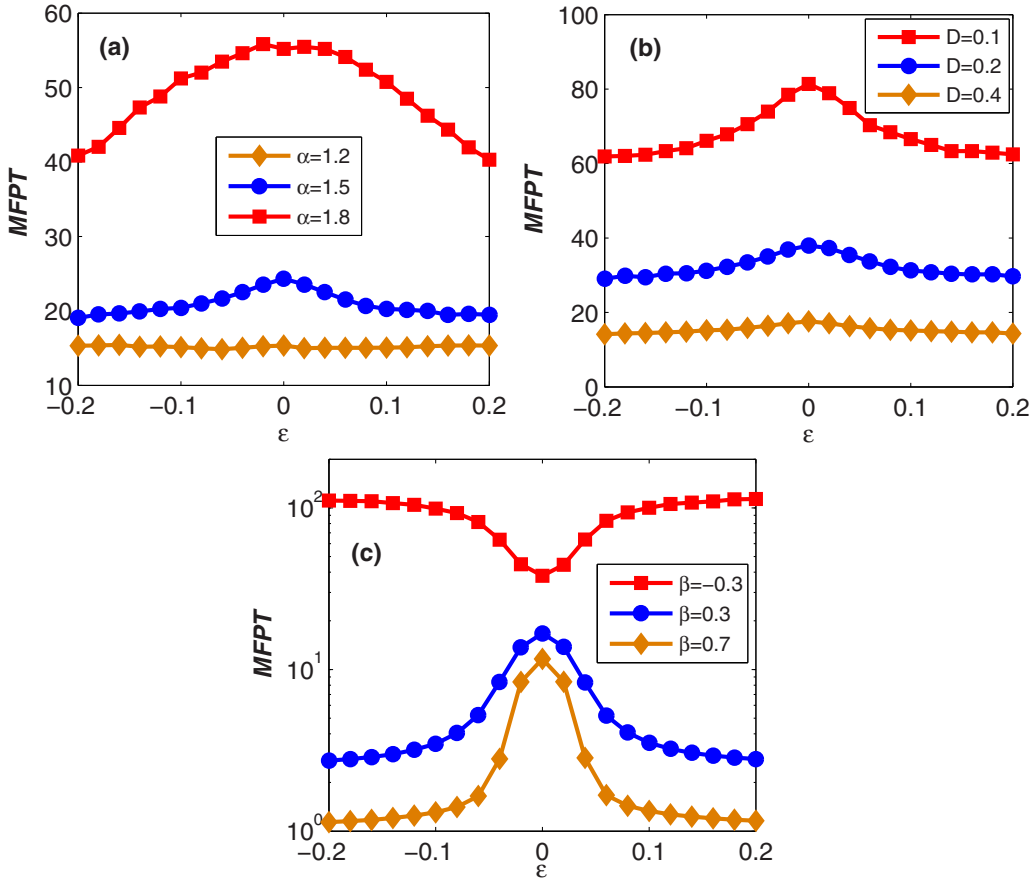


FIG. 7. MFPTs with respect to different amplitudes of the roughness in the potential. (a)  $\beta = 0$ ,  $D = 0.3$ , when  $\alpha = 1.2$  the MFPT is almost unchanged for varying  $\varepsilon$ , but when  $\alpha$  is large the roughness can decrease the MFPT significantly. (b)  $\alpha = 1.5$ ,  $\beta = 0$ , contrary to the case of  $\alpha$ , the MFPTs of small  $D$  acquires more influences from the roughness and decrease obviously. (c)  $\alpha = 1.5$ ,  $D = 0.3$ , for  $\beta > 0$ , roughness will decrease the MFPTs, but for  $\beta < 0$ , it is the opposite.

Different from  $\alpha$  and  $D$ , for  $\beta < 0$ , roughness does not accelerate the right crossing process as expected but prevents

it. As stated above, small perturbations benefit more from the roughness, while large jumps benefit less. For  $\beta < 0$ , most large excitations are on the left side leading to frequently negative excitations, which makes particles probably first jump to the left well at the beginning, except some special cases. When roughness is imposed, the match of large negative excitations and small minus noises will be much more powerful than positive small perturbations alone, resulting in more opportunities for particles to transfer from the middle well to the left well than smooth case, and thus it becomes even difficult to reach the right well. So we see roughness plays negative role for  $\beta < 0$ . For  $\beta > 0$ , Lévy distribution has a heavy right tail, so large positive excitations matching small perturbations makes it much easier to jump to the right well, as a result, roughness decreases the MFPTs.

V. SPLITTING PROBABILITY

The splitting probability is another important issue to describe the transition phenomenon. In a triple-well potential, when a particle starts from the middle well it may jump to either the left well or the right well. We use the splitting probability, which is the probability of a first escape from the middle well to the right or left, to elucidate the asymmetry of the first escape. So our aim in this section is to explore the laws of

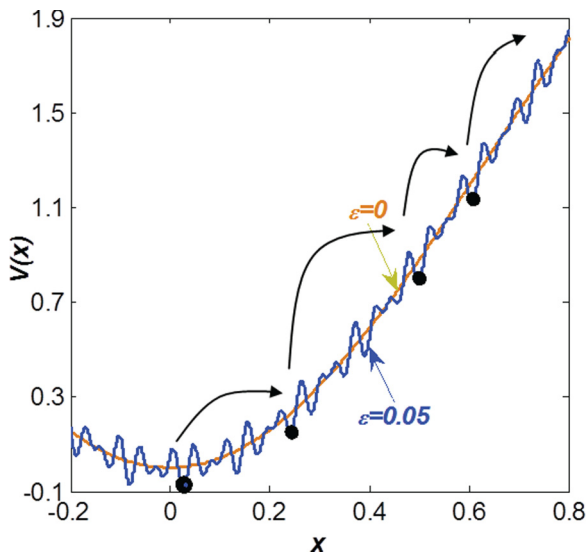


FIG. 8. The schematic illustration of the transitions for particles from rough potential well.

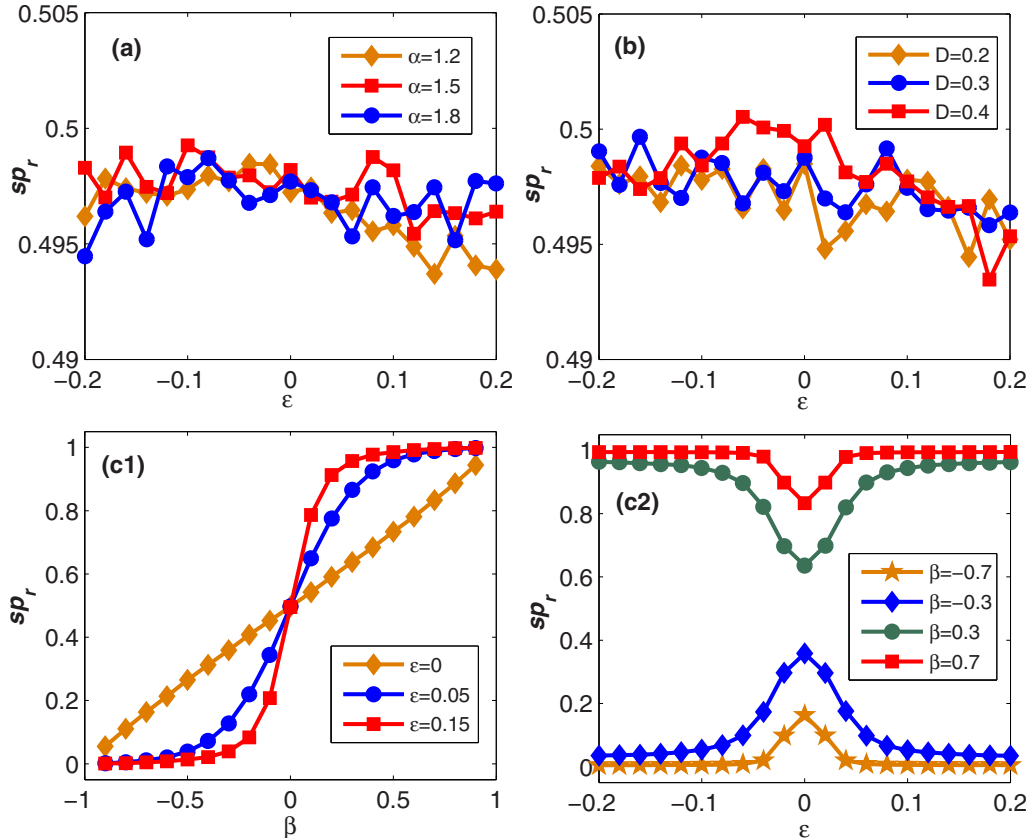


FIG. 9. The splitting probabilities from the middle well to the right well with respect to different amplitudes of roughness and  $\alpha$ ,  $\beta$ ,  $D$ . (a)  $\beta = 0$ ,  $D = 0.3$ ,  $sp_r$  for different  $\alpha$  change only a bit. (b)  $\alpha = 1.5$ ,  $\beta = 0$ , it is similar with  $\alpha$ , little change happens on different  $D$ . (c)  $\alpha = 1.5$ ,  $D = 0.3$ , the influences of roughness with respect  $\beta$  is significant, for  $\beta > 0$ , roughness will accelerate particles to jump to the right well, while for  $\beta < 0$ , roughness will weaken the process.

splitting from the middle well due to the interference of Lévy noise and roughness. Without loss of generality, we illustrate the splitting probability to the right side  $sp_r$ , defined by

$$sp_r = \lim_{N \rightarrow \infty} \frac{1}{N} \sum_{i=1}^N I_{A_i}(x_i), \quad (10)$$

$$A_i = \{x_i(\inf\{t : x_i(t) \leq x_{\min}^- \text{ OR } x_i(t) \geq x_{\min}^+\}) \geq x_{\min}^+\},$$

in which  $I_A(\cdot)$  is an indicator function.

In Figs. 9(a) and 9(b), we see the differences of  $sp_r$  due to different roughness with respect to  $\alpha$  and  $D$  are within the order of  $10^{-3}$ , which is such a small number that it can almost be neglected. However, it is a strong difference for  $\beta$  in Figs. 9(c1) and 9(c2). In the absence of roughness,  $sp_r(\varepsilon = 0)$  increases almost linearly, but when roughness is imposed,  $sp_r(\varepsilon)$  becomes totally nonlinear. We find that  $sp_r(\varepsilon) < sp_r(\varepsilon = 0)$  for  $\beta < 0$ , almost equal for  $\beta = 0$ , and  $sp_r(\varepsilon) > sp_r(\varepsilon = 0)$  for  $\beta > 0$ . A qualitative explanation of this phenomenon is similar to that of MFPTs under different  $\beta$ . As shown in Fig. 2, for  $\beta < 0$ , smaller  $\beta$  generate heavier left tails, which make it easier for particles to jump to the left, so that  $sp_r$  becomes smaller and smaller. Due to the roughness, small perturbations are activated to cooperate with large excitations leading to an even larger splitting rate to the left, and thus suppresses  $sp_r$ . While for  $\beta > 0$ , the match of small perturbations and large positive excitations further promotes

particles to jump to the right, so we see larger  $sp_r$  in rough cases. The effects is very significant near  $\beta = 0$ , that a small change of  $\beta$  leads to a large difference  $\Delta sp_r = 0.58$  between  $\beta = \pm 0.1$  for  $\varepsilon = 0.15$ . Along with the transformation of the sign of  $\beta$  is the inverse of which side has more large excitations, it is a small change but makes a big difference. Figure 9(c2) shows that the sign of roughness hardly changes  $sp_r$ , but with the increase of  $\varepsilon$ , the effects of roughness become more obvious.

## VI. CONCLUSION

Our study has demonstrated that a simple superimposed roughness on the smooth potential can produce lots of significant features in a triple-well system under Lévy noise. We have calculated the probability of a particle staying in the middle well, MFPT, and the splitting probability under different  $\varepsilon$  and Lévy parameters. We have shown that  $P_{\text{mid}}$  becomes remarkably smaller when roughness is introduced in the potential under the parameter of  $\beta$ , but very small differences occur under parameters  $\alpha$  and  $D$ , which says that skewed noises benefit much more from the roughness. Furthermore, we find that the roughness has an important enhancement effect on the transport of particles, that the easy become easier, the hard become harder. For the MFPT, we see larger roughness leads to less time to escape from



the middle well when  $\beta > 0$ , while it is opposite for  $\beta < 0$  that larger roughness lead longer MFPT. So we see if it is originally hard to cross the barriers it will be harder in the presence of roughness like  $\beta < 0$ , but if it is originally easy to escape, crossing will be easier under the interference of roughness like  $\beta > 0$  or common cases of  $\alpha$  and  $D$ . What's more, for large  $\alpha$  and small  $D$ , the enhancement effect on MFPT is more significant than small  $\alpha$  and large  $D$ . This is because small fluctuations get more advantages from the roughness than large jumps when particles try to escape from the middle well. Finally, for the splitting probability, it appears that small differences occur for parameters  $\alpha$  and  $D$ , because the enhancement effect on the transport is the same on both the right and left side, so when the noise is symmetric, although

roughness enhances the transport, there is no bias on both sides. But for asymmetric noise, when  $\beta > 0$  roughness speeds up the transport to the right, while when  $\beta < 0$  roughness slow down the right-side transport, so we see similar enhancement effect phenomenon for the splitting probability with different  $\beta$ .

## ACKNOWLEDGMENTS

This work was supported by the National Natural Science Foundation of China (Grant No. 11372247), the Fundamental Research Funds for the Central Universities, innovation foundation for doctor dissertation of NPU, and J.K. was supported by the Russian Science Foundation (Grant No. 16-12-10198).

- 
- [1] H. Frauenfelder, S. G. Sligar, and P. G. Wolynes, *Science* **254**, 1598 (1991).
- [2] A. Ansari, J. Berendzen, S. F. Bowne, H. Frauenfelder, I. E. Iben, T. B. Sauke, E. Shyamsunder, and R. D. Young, *Proc. Natl. Acad. Sci. U.S.A.* **82**, 5000 (1985).
- [3] L. Delemotte, M. A. Kasimova, M. L. Klein, M. Tarek, and V. Carnevale, *Proc. Natl. Acad. Sci. U.S.A.* **112**, 124 (2015).
- [4] T. Linder, B. L. de Groot, and A. Stary-Weinzinger, *PLoS Comput. Biol.* **9**, e1003058 (2013).
- [5] P. Charbonneau, J. Kurchan, G. Parisi, P. Urbani, and F. Zamponi, *Nat. Commun.* **5**, 3725 (2014).
- [6] J. C. Ye, J. Lu, C. T. Liu, Q. Wang, and Y. Yang, *Nat. Mater.* **9**, 619 (2010).
- [7] A. Heuer, B. Doliwa, and A. Saksengwitt, *Phys. Rev. E* **72**, 021503 (2005).
- [8] P. G. Debenedetti and F. H. Stillinger, *Nature* **410**, 259 (2001).
- [9] R. Zwanzig, *Proc. Natl. Acad. Sci. U.S.A.* **85**, 2029 (1988).
- [10] A. Ansari, *J. Chem. Phys.* **112**, 2516 (2000).
- [11] H. Frauenfelder, B. H. McMahon, R. H. Austin, K. Chu, and J. T. Groves, *Proc. Natl. Acad. Sci. U.S.A.* **98**, 2370 (2001).
- [12] C. Hyeon and D. Thirumalai, *Proc. Natl. Acad. Sci. U.S.A.* **100**, 10249 (2003).
- [13] R. Nevo, V. Brumfeld, R. Kapon, P. Hinterdorfer, and Z. Reich, *EMBO Rep.* **6**, 482 (2005).
- [14] L. Gammaitoni, P. Hänggi, P. Jung, and F. Marchesoni, *Rev. Mod. Phys.* **70**, 223 (1998).
- [15] R. Benzi, A. Sutera, and A. Vulpiani, *J. Phys. A: Math. Gen.* **14**, L453 (1981).
- [16] A. S. Pikovsky and J. Kurths, *Phys. Rev. Lett.* **78**, 775 (1997).
- [17] C. S. Zhou, J. Kurths, and B. Hu, *Phys. Rev. Lett.* **87**, 098101 (2001).
- [18] N. Namachchivaya, *Appl. Math. Comput.* **39**, 37 (1990).
- [19] Y. Xu, R. C. Gu, H. Q. Zhang, W. Xu, and J. Q. Duan, *Phys. Rev. E* **83**, 056215 (2011).
- [20] W. Horsthemke and R. Lefever, *Noise Induced Transition: Theory and Application in Physics, Chemistry, and Biology* (Springer, Berlin, 1984).
- [21] C. S. Zhou and J. Kurths, *Phys. Rev. Lett.* **88**, 230602 (2002).
- [22] V. I. Mel'nikov, *Phys. Rep.* **209**, 1 (1991).
- [23] P. Hanggi, P. Talkner, and M. Borkovec, *Rev. Mod. Phys.* **62**, 251 (1990).
- [24] J. Hasty, J. Pradines, M. Dolnik, and J. J. Collins, *Proc. Natl. Acad. Sci. U.S.A.* **97**, 2075 (1999).
- [25] S. Faetti, P. Grigolini, and F. Marchesoni, *Z. Phys. B-Condens. Mat.* **47**, 353 (1982).
- [26] D. Mondal, P. K. Ghosh, and D. S. Ray, *J. Chem. Phys.* **130**, 074703 (2009).
- [27] S. Banerjee, R. Biswas, K. Seki, and B. Bagchi, *J. Chem. Phys.* **141**, 124105 (2014).
- [28] S. Lifson and J. L. Jackson, *J. Chem. Phys.* **36**, 2410 (1962).
- [29] E. W. Montroll and G. H. Weiss, *J. Math. Phys.* **6**, 167 (1965).
- [30] Y. Xu, X. Q. Jin, and H. Q. Zhang, *Phys. Rev. E* **88**, 052721 (2013).
- [31] A. Koseska, A. Zaikin, J. García-Ojalvo, and J. Kurths, *Phys. Rev. E* **75**, 031917 (2007).
- [32] H.Y. Li, Z.H. Hou, and H.W. Xin, *Phys. Rev. E* **71**, 061916 (2005).
- [33] F. Moss and P. V. E. McClintock, *Noise in Nonlinear Dynamical Systems*, Vol. 2 (Cambridge University Press, New York, 1989).
- [34] Y. T. Lin and C. R. Doering, *Phys. Rev. E* **93**, 022409 (2016).
- [35] X. R. Shen, H. Zhang, Y. Xu, and S. X. Meng, *IEEE Sens. J.* **16**, 1998 (2016).
- [36] P. D. Ditlevsen, *Geophys. Res. Lett.* **26**, 1441 (1999).
- [37] A. Singh and M. Soltani, *PLoS ONE* **8**, e84301 (2013).
- [38] B. Munsky, G. Neuert, and A. Oudenaarden, *Science* **336**, 183 (2012).
- [39] F. Matthäus, M. S. Mommer, T. Curk, and J. Dobnikar, *PLoS ONE* **6**, e18623 (2011).
- [40] P. Barthelemy, J. Bertolotti, and D. S. Wiersma, *Nature* **453**, 495 (2008).
- [41] Á. Corral, *Phys. Rev. Lett.* **97**, 178501 (2006).
- [42] I. Pavlyukevich, *Stoch. Dynam.* **11**, 495 (2011).
- [43] H. Risken, *The Fokker-Planck Equation: Methods of Solution and Applications* (Springer, Berlin, 1984).
- [44] A. V. Chechkin, J. Klafter, V. Y. Gonchar, R. Metzler, and L. V. Tanatarov, *Phys. Rev. E* **67**, 010102(R) (2003).